International Journal of Smart and Nano Materials

Publication details, including instructions for authors and subscription information:
http://www.tandfonline.com/loi/tsnm20

Fatigue analysis of piezoelectric microdevice based on a continuum damage model

Xianqiao Wang[a] & Ken P. Chong[b]

[a] College of Engineering, University of Georgia, Athens 30606, GA, USA

[b] Department of Mechanical and Aerospace Engineering, George Washington University, Washington 20052, DC, USA

Published online: 18 Sep 2013.

To cite this article: Xianqiao Wang & Ken P. Chong , International Journal of Smart and Nano Materials (2013): Fatigue analysis of piezoelectric microdevice based on a continuum damage model, International Journal of Smart and Nano Materials, DOI: 10.1080/19475411.2013.837107

To link to this article: http://dx.doi.org/10.1080/19475411.2013.837107

International Journal of Smart and Nano Materials, 2013
http://dx.doi.org/10.1080/19475411.2013.837107

Taylor & Francis
Taylor & Francis Group

Fatigue analysis of piezoelectric microdevice based on a continuum damage model

Xianqiao Wang[a]* and Ken P. Chong[b]

[a]*College of Engineering, University of Georgia, Athens 30606, GA, USA;* [b]*Department of Mechanical and Aerospace Engineering, George Washington University, Washington 20052, DC, USA*

(*Received 6 July 2013; final version received 19 August 2013*)

The utilization of piezoelectric materials in MEMS devices under harsh environments has gained affordable appreciations due to its unique mechanical and electrical material properties. However, the reliability of MEMS devices triggered by fatigue damage remains elusive and needs to be further explored. Here, we present a continuum constitutive model for piezoelectric materials containing a substantive amount of randomly dispersed microcracks. The constitutive equation of the piezoelectric materials with microcracks is formulated via Helmholtz free energy by combining the Kachanvo damage evolution law and the Chaboche fatigue damage development to express the fatigue damage growth. A case of the fatigue damage analysis of the piezoelectric microplate with transverse matrix cracks in the status of plane stress is presented by adopting the von Karman's plate theory. With numerical schemes employed, the effect of cyclic impulsive loadings and electrical loadings on the fatigue damage and fatigue life prediction of a piezoelectric microplate is investigated and discussed. The findings provide valuable insights into the fundamental mechanism of reliability in piezoelectric MEMS devices due to cyclic loadings, thereby offering new ways to exploit and fabricate the piezoelectric-based MEMS devices suitable for harsh conditions.

Keywords: piezoelectric microplate; constitutive equation; fatigue analysis; MEMS; cyclic loading

1. Introduction

The converging interdisciplinary areas of micro-electro-mechanical systems (MEMS), nanotechnology, biotechnology, information technology, and cognitive science, offer the potential of improving human lives, as well as the well-being and productivity of society [1]. Simulation-based engineering science has emerged as a powerful tool revolutionizing engineering and science in the twenty-first century [2]. It plays a major role in multi-scale material modeling and system design, including MEMS. The use of piezoelectric materials has received considerable attention in intelligent structures due to its intrinsic, direct, and converse piezoelectric effects in recent years. Piezoelectric materials have been utilized in MEMS devices as sensors or actuators for the control of active shape or vibration of the structures. Defects, such as micro cracks, voids, dislocations, and delamination, are introduced in the piezoelectric materials during manufacturing and poling process.

*Corresponding author. Email: xqwang@uga.edu
Ken P. Chong is also a NIST Associate.

The existence of these defects greatly affects the electric, dielectric, elastic, mechanical, and piezoelectric properties of the piezoelectric materials, especially the service life of piezoelectric microstructures. When subjected to cyclic mechanical and electrical loads, these defects may grow in size and cracks may propagate leading to the premature mechanical or electrical fatigue failure of the piezoelectric microstructures. Therefore, it is important to understand the growth of these defects, the fatigue damage accumulation, and the overall effect of these defects on the average mechanical and electrical properties of piezoelectric microstructures so that reliable service life predictions of the structure can be evaluated. Analysis of such situations is yet to be reliably accomplished and progress depends on our ability to formulate constitutive relationships for anisotropic piezoelectric materials incorporating deformation and randomly distributed defects.

Fatigue damage in fiber-reinforced composite materials has been vastly investigated, and many theories have been established and employed to predict the life of composite structures. Many researchers have investigated the behaviors of laminated composites under static/dynamic loads and cyclic loads [3–5]. Most of these fatigue studies are experimental, and have added to the understanding of the mechanisms involved in the fatiguing of composites. Some have even developed design methodologies, and an extensive list of these can be found in a paper by Nyman [6], which also describes a simplified fatigue design approach about composite materials. Dahlen and Springer [7] proposed a semi-empirical model for estimating delamination growth in graphite/epoxy laminates under cyclic loads. Feng [8] developed a model for predicting fatigue damage growth in carbon fiber-reinforced specimens due to matrix cracking.

Modeling and analysis of multilayer piezoelectric beams and plates have reached a relative maturity as attested by numerous papers. Mindlin [9] presented the theory of the mode of piezoelectric crystals plate considering shear and bending. Tiersten [10] developed general piezoelectric nonlinear theory and detailed the vibration equations of different piezoelectric crystals. Chandrashekhara and Tenneti [11] and Zhou [12] investigated the dynamic control of laminated piezoelectric plates by finite element (FE) method. Wang and Rogers [13] presented a model based on classical plate theory for laminated plates with spatially distributed piezoelectric patches. Tzou and Gadre [14] analyzed thin laminates coupled with shell actuators for distributed vibration control. Xu [15] analyzed the free vibration of laminated piezothermoelectric plate based on the 3D theory. Mitchell and Reddy [16] proposed the theory of laminated piezoelectric plates by using classical plate theory and simple third-order theory, respectively. Rao and Sunar [17] developed a FE formulation of piezothermoelastic media and integrated it with the distributed sensing and control of intelligent structures. Tauchert [18] applied Nowacki's general theory to piezothermoelastic laminated plates and obtained the static solutions. However, up to now, the analysis of static/dynamic and fatigue life problems for the piezoelectric microstructures, considering the damage effects under cyclic loading are still lacking.

In this article, a new constitutive model for piezoelectric materials is presented by using the Talreja's tensor-valued internal state damage variables and the Helmholtz free energy of piezoelectric materials. This model is applied to a specific case of fatigue damage analysis of piezoelectric plates under cyclic impulsive loading. By adopting von Karman's plate theory and using numerical scheme, the effect of cyclic impulsive loading and electric loads on the fatigue damage analysis and fatigue life prediction of the piezoelectric microplate are investigated and discussed.

2. Basic equations

2.1. Constitutive equations for damaged piezoelectric materials

Consider a representative volume element of a piezoelectric material with a multitude of damage entities in the form of micro cracks, as shown in Figure 1. As discussed in Talreja [19], two vectors are needed to define each damage entity. These are damage influence vector $\overrightarrow{a_i}$ and unit normal $\overrightarrow{n_i}$ to damage entity surface. Damage influence vector represents an appropriately chosen effect of damage entity on the surrounding medium. With these two vectors, a damage entity tensor d_{ij} is formed by taking an integral of the diad $\overrightarrow{a_i}\ \overrightarrow{n_j}$ over the surface of the damage entity.

$$d_{ij} = \int_S \overrightarrow{a_i}\ \overrightarrow{n_j}\,\mathrm{d}S \tag{1}$$

Now, if there are $n$distinct damage modes in the representative volume element (e.g., intralaminar crack in different orientations etc.), denoted by$k = 1, 2, \ldots n$, a damage tensor can be defined for each mode as

$$\omega_{ij}^k = \frac{1}{V_r}\sum_{\vartheta_k}(d_{ij})_{\vartheta_k} \tag{2}$$

where V_r is the volume of the representative volume element and ϑ_k represents the number of damage entities in the kth damage mode. The tensor ω_{ij}^k is an asymmetric tensor in general. However, we can represent the vector $\overrightarrow{a_i}$ along the normal and tangential directions at any point on the surface of the damage entity and write

$$d_{ij} = d_{ij}^1 + d_{ij}^2 \tag{3}$$

where $d_{ij}^1 = \int_S \overrightarrow{an_i}\ \overrightarrow{n_j}\,\mathrm{d}S$ and $d_{ij}^2 = \int_S \overrightarrow{bm_i}\ \overrightarrow{n_j}\,\mathrm{d}S$. a and b are the magnitudes of the normal and tangential projections of vector $\overrightarrow{a_i}$, respectively, and vectors $\overrightarrow{n_i}$ and $\overrightarrow{m_i}$ are unit normal and tangential vectors, respectively. Thus, the damage tensor ω_{ij} can be written as

$$\omega_{ij}^k = \omega_{ij}^{1k} + \omega_{ij}^{2k} \tag{4}$$

where $\omega_{ij}^{1k} = \frac{1}{V_r}\sum_{\vartheta_k}(d_{ij}^1)_{\vartheta_k}$ and $\omega_{ij}^{2k} = \frac{1}{V_r}\sum_{\vartheta_k}(d_{ij}^2)_{\vartheta_k}$

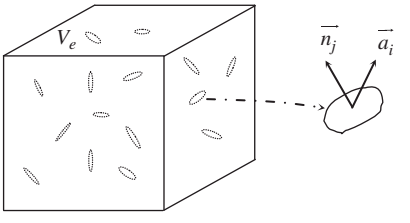

Figure 1. Representative volume element with internal damage variables for piezoelectric materials.

Physically, the damage tensor ω_{ij}^{1k} represents the effects of crack opening on the surrounding medium, whereas the damage tensor ω_{ij}^{2k} represents the effects of sliding between the two crack faces. In many situations, the sliding between the crack faces can be negligible, e.g., for intralaminar cracks constrained by stiff plies, and hence we assume $\omega_{ij}^{2k} \equiv 0$. This implies $\omega_{ij}^{k} \equiv \omega_{ij}^{1k}$, which is a symmetric tensor.

For the case of damaged piezoelectric material without temperature effect where the damage is represented by internal state variables, the Helmholtz free energy of piezoelectric material can be written as a function of the transformed elastic strains, the electric field vector, and damage internal variables, that is

$$H = H(\varepsilon_{ij},\ E_i,\ \omega_{ij}^{k}) \tag{5}$$

The transformed stress components σ_{ij} and the electric displacement components G_i at any fixed damage state are now given by

$$\sigma_{ij} = \frac{\partial H(\varepsilon_{ij},\ E_i,\ \omega_{ij}^{k})}{\partial \varepsilon_{ij}}$$

$$G_i = -\frac{\partial H(\varepsilon_{ij},\ E_i,\ \omega_{ij}^{k})}{\partial E_i} \tag{6}$$

Here, we assume the damage induced by the cracks in the piezoelectric material has the orthotropic property, the irreducible integrity bases for a scalar polynomial function of two symmetric second-rank tensors can be expressed as [20]:

$$\begin{aligned}
&\varepsilon_{11},\ \varepsilon_{22},\ \varepsilon_{33},\ {\varepsilon_{23}}^2,\ {\varepsilon_{31}}^2,\ {\varepsilon_{12}}^2,\ \varepsilon_{12}\varepsilon_{23}\varepsilon_{31},\\
&\omega_{11}^{k},\ \omega_{22}^{k},\ \omega_{33}^{k},\ (\omega_{23}^{k})^2,\ (\omega_{31}^{k})^2,\ (\omega_{12}^{k})^2,\ \omega_{12}^{k}\omega_{23}^{k}\omega_{31}^{k}\\
&\varepsilon_{23}\omega_{23}^{k},\ \varepsilon_{31}\omega_{31}^{k},\ \varepsilon_{12}\omega_{12}^{k},\ \omega_{23}^{k}\varepsilon_{12}\varepsilon_{13},\ \omega_{31}^{k}\varepsilon_{32}\varepsilon_{12},\ \omega_{12}^{k}\varepsilon_{13}\varepsilon_{23}, \qquad (k = 1, 2, \cdots n)\\
&\varepsilon_{23}\omega_{12}^{k}\omega_{13}^{k},\ \varepsilon_{31}\omega_{32}^{k}\omega_{12}^{k},\ \varepsilon_{12}\omega_{13}^{k}\omega_{23}^{k}\\
&E_1,\ E_2,\ E_3
\end{aligned} \tag{7}$$

where n is the number of the cracks' direction in the material.

For a piezoelectric single-layer microplate, the local coordinate system $o - 123$ is selected, in which 1 and 2 denote the two principal directions of the piezoelectric plate, 3 is vertical to the midsurface. According to Kirchhoff hypothesis, for plate $\varepsilon_{13} = \varepsilon_{23} = 0$ and applying Voigt notation to describe strains and damage variables, the bases of invariants can be further written as

$$\begin{aligned}
&\varepsilon_1,\ \varepsilon_2,\ \varepsilon_3,\ \varepsilon_6^2,\ \omega_1^{k},\ \omega_2^{k},\ \omega_3^{k},\ (\omega_4^{k})^2,\ (\omega_5^{k})^2,\ (\omega_6^{k})^2,\\
&\omega_4^{k}\omega_5^{k}\omega_6^{k},\ \varepsilon_6\omega_6^{k},\ \varepsilon_6\omega_4^{k}\omega_5^{k} \qquad (k = 1, 2, \cdots n)\\
&E_1,\ E_2,\ E_3
\end{aligned} \tag{8}$$

Using the above-stated irreducible integrity bases, the Helmholtz free energy of piezoelectric materials can be expressed as a quadratic expression of the strains or the electric field intensity, a mixture quadratic expression of strains and electric field intensity, and a linear expression of damage variables [21] as follows

$$
\begin{aligned}
H = {} & C_1^0\varepsilon_1^2 + C_2^0\varepsilon_1\varepsilon_2 + C_3^0\varepsilon_2^2 + C_4^0\varepsilon_6^2 + C_5^0\varepsilon_1^2 + C_6^0\varepsilon_1\varepsilon_3 + C_7^0\varepsilon_2\varepsilon_3 - (\kappa_1^0E_1^2 + \kappa_2^0E_2^2 \\
& + \kappa_3^0E_3^2 + \kappa_4^0E_1E_2 + \kappa_5^0E_2E_3 + \kappa_6^0E_3E_1) - (e_1^0E_1\varepsilon_1 + e_2^0E_1\varepsilon_2 + e_3^0E_1\varepsilon_3 + e_4^0E_2\varepsilon_1 \\
& + e_5^0E_2\varepsilon_2 + e_6^0E_2\varepsilon_3 + e_7^0E_3\varepsilon_1 + e_8^0E_3\varepsilon_2 + e_9^0E_3\varepsilon_3) + \sum_{k=1}^{n}\Big(C_1^k\varepsilon_1^2\omega_1^k + C_2^k\varepsilon_1^2\omega_2^k + C_3^k\varepsilon_1^2\omega_3^k \\
& + C_4^k\varepsilon_2^2\omega_1^k + C_5^k\varepsilon_2^2\omega_2^k + C_6^k\varepsilon_2^2\omega_3^k + C_7^k\varepsilon_3^2\omega_1^k + C_8^k\varepsilon_3^2\omega_2^k + C_9^k\varepsilon_3^2\omega_3^k + C_{10}^k\varepsilon_6^2\omega_1^k \\
& + C_{11}^k\varepsilon_6^2\omega_2^k + C_{12}^k\varepsilon_6^2\omega_3^k + C_{13}^k\varepsilon_1\varepsilon_2\omega_1^k + C_{14}^k\varepsilon_1\varepsilon_2\omega_2^k + C_{15}^k\varepsilon_1\varepsilon_2\omega_3^k + C_{16}^k\varepsilon_2\varepsilon_3\omega_1^k \\
& + C_{17}^k\varepsilon_2\varepsilon_3\omega_2^k + C_{18}^k\varepsilon_2\varepsilon_3\omega_3^k + C_{19}^k\varepsilon_3\varepsilon_1\omega_1^k + C_{20}^k\varepsilon_3\varepsilon_1\omega_2^k + C_{21}^k\varepsilon_3\varepsilon_1\omega_3^k + C_{22}^k\varepsilon_6\varepsilon_1\omega_6^k \\
& + C_{23}^k\varepsilon_6\varepsilon_2\omega_6^k + C_{24}^k\varepsilon_6\varepsilon_3\omega_6^k\Big) - \sum_{k=1}^{n}\Big(\kappa_1^kE_1^2\omega_1^k + \kappa_2^kE_1^2\omega_2^k + \kappa_3^kE_1^2\omega_3^k + \kappa_4^kE_2^2\omega_1^k + \kappa_5^kE_2^2\omega_2^k \\
& + \kappa_6^kE_3^2\omega_3^k + \kappa_7^kE_3^2\omega_1^k + \kappa_8^kE_3^2\omega_2^k + \kappa_9^kE_3^2\omega_3^k + \kappa_{10}^kE_1E_2\omega_1^k + \kappa_{11}^kE_1E_2\omega_2^k + \kappa_{12}^kE_1E_2\omega_3^k \\
& + \kappa_{13}^kE_2E_3\omega_1^k + \kappa_{14}^kE_2E_3\omega_2^k + \kappa_{15}^kE_2E_3\omega_3^k + \kappa_{16}^kE_3E_1\omega_1^k + \kappa_{17}^kE_3E_1\omega_2^k + \kappa_{18}^kE_3E_1\omega_3^k\Big) \\
& - \sum_{k=1}^{n}\Big(e_1^kE_1\varepsilon_1\omega_1^k + e_2^kE_1\varepsilon_1\omega_2^k + e_3^kE_1\varepsilon_1\omega_3^k + e_4^kE_1\varepsilon_2\omega_1^k + e_5^kE_1\varepsilon_2\omega_2^k + e_6^kE_1\varepsilon_2\omega_3^k \\
& + e_7^kE_1\varepsilon_3\omega_1^k + e_8^kE_1\varepsilon_3\omega_2^k + e_9^kE_1\varepsilon_3\omega_3^k + e_{10}^kE_2\varepsilon_1\omega_1^k + e_{11}^kE_2\varepsilon_1\omega_2^k + e_{12}^kE_2\varepsilon_1\omega_3^k \\
& + e_{13}^kE_2\varepsilon_2\omega_1^k + e_{14}^kE_2\varepsilon_2\omega_2^k + e_{15}^kE_2\varepsilon_2\omega_3^k + e_{16}^kE_2\varepsilon_3\omega_1^k + e_{17}^kE_2\varepsilon_3\omega_2^k + e_{18}^kE_2\varepsilon_3\omega_3^k \\
& + e_{19}^kE_3\varepsilon_1\omega_1^k + e_{20}^kE_3\varepsilon_1\omega_2^k + e_{21}^kE_3\varepsilon_1\omega_3^k + e_{22}^kE_3\varepsilon_2\omega_1^k + e_{23}^kE_3\varepsilon_2\omega_2^k + e_{24}^kE_3\varepsilon_2\omega_3^k \\
& + e_{25}^kE_3\varepsilon_3\omega_1^k + e_{26}^kE_3\varepsilon_3\omega_2^k + e_{27}^kE_3\varepsilon_3\omega_3^k + e_{28}^kE_1\varepsilon_6\omega_6^k + e_{29}^kE_2\varepsilon_6\omega_6^k + e_{30}^kE_3\varepsilon_6\omega_6^k\Big) \\
& + P_0 + P_1\left(\varepsilon_p, \omega_q^k\right) + P_2\left(\omega_q^k\right) + P_3\left(E_i, \omega_q^k\right) \qquad (9)
\end{aligned}
$$

where $C_i^0(i = 1, 2, \cdots 7)$ are the elastic material constants without damage, $e_i^0(i = 1, 2, \cdots 9)$ are the piezoelectric constants without damage, $\kappa_i^0(i = 1, 2, \cdots 6)$ are the permittivity matrix constants without damage, $C_i^k(i = 1, 2, \cdots 24)$ are the material constants with damage, $e_i^k(i = 1, 2, \cdots 30)$ are the piezoelectric constants with damage, $\kappa_i^k(i = 1, 2, \cdots 18)$ are the permittivity matrix constants with damage, ρ is the density of piezoelectric material, P_0 is a constant, P_1 is a linear function of strains, P_2 is a linear function of damage variables, and P_3 is a linear function of the electric field intensity. Then the stresses and the electric displacements can be expressed as

$$\sigma_p = \frac{\partial H}{\partial \varepsilon_p} = \left[C_{pq}^0 + \sum_{k=1}^{n} C_{pq}^k \right] \varepsilon_q - \left[e_{pm}^0 + \sum_{k=1}^{n} e_{pm}^k \right] E_m$$

$$G_m = -\frac{\partial H}{\partial E_m} = \left[e_{qm}^0 + \sum_{k=1}^{n} e_{qm}^k \right]^T \varepsilon_q + \left[\kappa_{mn}^0 + \sum_{k=1}^{n} \kappa_{mn}^k \right] E_n \tag{10}$$

where C_{pq}^0, C_{pq}^k, κ_{mn}^0, and κ_{mn}^k are all symmetric matrices having the forms as follows:

$$[C_{pq}^0] = \begin{bmatrix} 2C_1^0 & C_2^0 & C_6^0 & 0 \\ & 2C_3^0 & C_7^0 & 0 \\ & & 2C_5^0 & 0 \\ & & & 2C_4^0 \end{bmatrix} \tag{11}$$

$$[C_{pq}^k] = \begin{bmatrix} 2C_1^k\omega_1^k + 2C_2^k\omega_2^k + 2C_3^k\omega_3^k & C_{13}^k\omega_1^k + C_{14}^k\omega_2^k + C_{15}^k\omega_3^k \\ & 2C_4^k\omega_1^k + 2C_5^k\omega_2^k + 2C_6^k\omega_3^k \\ & \\ C_{19}^k\omega_1^k + C_{20}^k\omega_2^k + C_{21}^k\omega_3^k & C_{22}^k\omega_6^k \\ C_{16}^k\omega_1^k + C_{17}^k\omega_2^k + C_{18}^k\omega_3^k & C_{23}^k\omega_6^k \\ 2C_7^k\omega_1^k + 2C_8^k\omega_2^k + 2C_9^k\omega_3^k & C_{24}^k\omega_6^k \\ & 2C_{10}^k\omega_1^k + 2C_{11}^k\omega_2^k + 2C_{12}^k\omega_3^k \end{bmatrix} \tag{12}$$

$$[e_{pm}^0] = \begin{bmatrix} e_1^0 & e_4^0 & e_7^0 \\ e_2^0 & e_5^0 & e_8^0 \\ e_3^0 & e_6^0 & e_9^0 \\ 0 & 0 & 0 \end{bmatrix} \tag{13}$$

$$[\kappa_{mn}^0] = \begin{bmatrix} 2\kappa_1^0 & \kappa_4^0 & \kappa_6^0 \\ & 2\kappa_2^0 & \kappa_5^0 \\ & & 2\kappa_3^0 \end{bmatrix} \tag{14}$$

$$[e_{pm}^k] = \begin{bmatrix} e_1^k\omega_1^k + e_2^k\omega_2^k + e_3^k\omega_3^k & e_{10}^k\omega_1^k + e_{11}^k\omega_2^k + e_{12}^k\omega_3^k & e_{19}^k\omega_1^k + e_{20}^k\omega_2^k + e_{21}^k\omega_3^k \\ e_4^k\omega_1^k + e_5^k\omega_2^k + e_6^k\omega_3^k & e_{13}^k\omega_1^k + e_{14}^k\omega_2^k + e_{15}^k\omega_3^k & e_{22}^k\omega_1^k + e_{23}^k\omega_2^k + e_{24}^k\omega_3^k \\ e_7^k\omega_1^k + e_8^k\omega_2^k + e_9^k\omega_3^k & e_{16}^k\omega_1^k + e_{17}^k\omega_2^k + e_{18}^k\omega_3^k & e_{25}^k\omega_1^k + e_{26}^k\omega_2^k + e_{27}^k\omega_3^k \\ e_{28}^k\omega_6^k & e_{29}^k\omega_6^k & e_{30}^k\omega_6^k \end{bmatrix} \tag{15}$$

$$[\kappa_{mn}^k] = \begin{bmatrix} 2\kappa_1^k\omega_1^k + 2\kappa_2^k\omega_2^k + 2\kappa_3^k\omega_3^k & \kappa_{10}^k\omega_1^k + \kappa_{11}^k\omega_2^k + \kappa_{12}^k\omega_3^k & \kappa_{16}^k\omega_1^k + \kappa_{17}^k\omega_2^k + \kappa_{18}^k\omega_3^k \\ & 2\kappa_4^k\omega_1^k + 2\kappa_5^k\omega_2^k + 2\kappa_6^k\omega_3^k & \kappa_{13}^k\omega_1^k + \kappa_{14}^k\omega_2^k + \kappa_{15}^k\omega_3^k \\ & & 2\kappa_7^k\omega_1^k + 2\kappa_8^k\omega_2^k + 2\kappa_9^k\omega_3^k \end{bmatrix} \tag{16}$$

Assuming that there is only one damage mode in the representative volume element, the relations of the strains, the stresses, the electric field intensity, and the electric displacements in Equation (10) can be simplified as

$$\sigma_p = [C^0_{pq} + C^1_{pq}]\varepsilon_q - [e^0_{pm} + e^1_{pm}]E_m$$
$$G_m = [e^0_{qm} + e^1_{qm}]^T\varepsilon_q + [\kappa^0_{mn} + \kappa^1_{mn}]E_n \tag{17}$$

where C^0_{pq}, e^0_{pm}, and κ^0_{mn} are same as before. C^k_{pq}, e^k_{pm}, and κ^k_{mn} are replaced by C^1_{pq}, e^1_{pm}, and κ^1_{mn}, respectively.

In present study, consider that the cracks in the piezoelectric plate are parallel to the coordinate plane 1–3, all damage variables, except ω_2, are zero. Then the coefficient matrices in Equations (12), (15), and (16) can be simplified as

$$[C^1_{pq}] = \begin{bmatrix} 2C_2\omega_2 & C_{14}\omega_2 & C_{20}\omega_2 & 0 \\ & 2C_5\omega_2 & C_{17}\omega_2 & 0 \\ & & 2C_8\omega_2 & 0 \\ & & & 2C_{11}\omega_2 \end{bmatrix} \tag{18}$$

$$[e^1_{pm}] = \begin{bmatrix} e_2\omega_2 & e_{11}\omega_2 & e_{20}\omega_2 \\ e_5\omega_2 & e_{14}\omega_2 & e_{23}\omega_2 \\ e_8\omega_2 & e_{17}\omega_2 & e_{26}\omega_2 \\ 0 & 0 & 0 \end{bmatrix} \tag{19}$$

$$[\kappa^1_{mn}] = \begin{bmatrix} 2\kappa_2\omega_2 & \kappa_{11}\omega_2 & \kappa_{17}\omega_2 \\ & 2\kappa_5\omega_2 & \kappa_{14}\omega_2 \\ & & 2\kappa_8\omega_2 \end{bmatrix} \tag{20}$$

Since cracks are parallel to the coordinate plane 1–3, the effect of the damage on the plate stiffness in this coordinate plane 1–3 can be neglected, which means that the components C^1_{11} and C^1_{33} of stiffness matrix due to damage effect are negligible. Then matrix in Equation (18) can be further simplified as

$$[C^1_{pq}] = \begin{bmatrix} 0 & C_{14}\omega_2 & C_{20}\omega_2 & 0 \\ & 2C_5\omega_2 & C_{17}\omega_2 & 0 \\ & & 0 & 0 \\ & & & 2C_{11}\omega_2 \end{bmatrix} \tag{21}$$

Assuming $\sigma_3 = 0$ and using Equation (17), the constitutive relations with damage of the piezoelectric plate for the plane stress problems are obtained as follows:

$$\sigma_p = [C_{pq}]\varepsilon_q - [e_{pm}]E_m = [C^0_{pq} + C^1_{pq}]\varepsilon_q - [e^0_{pm} + e^1_{pm}]E_m$$
$$G_m = [e_{qm}]^T\varepsilon_q + [\kappa_{mn}]E_n = [e^0_{qm} + e^1_{qm}]^T\varepsilon_q + [\kappa^0_{mn} + \kappa^1_{mn}]E_n \quad (p, q = 1, 2, 6 \quad m, n = 1, 2, 3) \tag{22}$$

where

$$[C^0_{pq}] = \begin{bmatrix} 2C^0_1 - \frac{(C^0_6)^2}{2C^0_5} & C^0_2 - \frac{C^0_6 C^0_7}{2C^0_5} & 0 \\ & 2C^0_3 - \frac{(C^0_7)^2}{2C^0_5} & 0 \\ & & 2C^0_4 \end{bmatrix} \underline{\underline{def}} \begin{bmatrix} C^*_{11} & C^*_{12} & 0 \\ & C^*_{22} & 0 \\ & & C^*_{66} \end{bmatrix} \tag{23}$$

$$[C^1_{pq}] = \begin{bmatrix} \frac{C^0_6 C_{20}\omega_2}{C^0_5} & \left(C_{14} - \frac{C^0_7 C_{20} + C^0_6 C_{17}}{2C^0_5}\right)\omega_2 & 0 \\ & \left(2C_5 - \frac{C^0_7 C_{17}}{C^0_5}\right)\omega_2 & 0 \\ & & 2C_{11}\omega_2 \end{bmatrix} \underline{\underline{def}} \begin{bmatrix} \alpha_{11} & \alpha_{12} & 0 \\ & \alpha_{22} & 0 \\ & & \alpha_{66} \end{bmatrix} \omega_2 \tag{24}$$

$$[e^0_{pm}] = \begin{bmatrix} e^0_1 - \frac{C^0_6 e^0_3}{2C^0_5} & e^0_4 - \frac{C^0_6 e^0_6}{2C^0_5} & e^0_7 - \frac{C^0_6 e^0_9}{2C^0_5} \\ e^0_2 - \frac{C^0_7 e^0_3}{2C^0_5} & e^0_5 - \frac{C^0_7 e^0_6}{2C^0_5} & e^0_8 - \frac{C^0_7 e^0_9}{2C^0_5} \\ 0 & 0 & 0 \end{bmatrix} \underline{\underline{def}} \begin{bmatrix} e^*_{11} & e^*_{12} & e^*_{13} \\ e^*_{21} & e^*_{22} & e^*_{23} \\ 0 & 0 & 0 \end{bmatrix} \tag{25}$$

$$[e^1_{pm}] = \begin{bmatrix} \left(e_2 - \frac{C^0_6 e_8 + C_{20} e^0_3}{2C^0_5}\right)\omega_2 & \left(e_{11} - \frac{C^0_6 e_{17} + C_{20} e^0_6}{2C^0_5}\right)\omega_2 & \left(e_{20} - \frac{C^0_6 e_{26} + C_{20} e^0_9}{2C^0_5}\right)\omega_2 \\ \left(e_5 - \frac{C^0_7 e_8 + C_{17} e^0_3}{2C^0_5}\right)\omega_2 & \left(e_{14} - \frac{C^0_6 e_{17} + C_{17} e^0_6}{2C^0_5}\right)\omega_2 & \left(e_{23} - \frac{C^0_7 e_{26} + C_{17} e^0_9}{2C^0_5}\right)\omega_2 \\ 0 & 0 & 0 \end{bmatrix}$$

$$\underline{\underline{def}} \begin{bmatrix} \beta_{11} & \beta_{12} & \beta_{13} \\ \beta_{21} & \beta_{22} & \beta_{23} \\ 0 & 0 & 0 \end{bmatrix} \omega_2 \tag{26}$$

$$[\kappa^0_{mn}] = \begin{bmatrix} 2\kappa^0_1 + \frac{(e^0_3)^2}{2C^0_5} & \kappa^0_4 + \frac{e^0_3 e^0_6}{2C^0_5} & \kappa^0_6 + \frac{e^0_3 e^0_9}{2C^0_5} \\ & 2\kappa^0_2 + \frac{(e^0_6)^2}{2C^0_5} & \kappa^0_5 + \frac{e^0_6 e^0_9}{2C^0_5} \\ & & 2\kappa^0_3 + \frac{(e^0_9)^2}{2C^0_5} \end{bmatrix} \underline{\underline{def}} \begin{bmatrix} \kappa^*_{11} & \kappa^*_{12} & \kappa^*_{13} \\ & \kappa^*_{22} & \kappa^*_{23} \\ & & \kappa^*_{33} \end{bmatrix} \tag{27}$$

$$[\kappa^1_{mn}] = \begin{bmatrix} \left(2\kappa_2 + \frac{e^0_3 e_8}{C^0_5}\right)\omega_2 & \left(\kappa_{11} + \frac{e^0_3 e_{17} + e^0_6 e_8}{2C^0_5}\right)\omega_2 & \left(\kappa_{17} + \frac{e^0_3 e_{26} + e^0_9 e_8}{2C^0_5}\right)\omega_2 \\ & \left(2\kappa_5 + \frac{e^0_6 e_{17}}{C^0_5}\right)\omega_2 & \left(\kappa_{14} + \frac{e^0_6 e_{26} + e^0_9 e_{17}}{2C^0_5}\right)\omega_2 \\ & & \left(2\kappa_8 + \frac{e^0_9 e_{26}}{C^0_5}\right)\omega_2 \end{bmatrix}$$

$$\underline{\underline{def}} \begin{bmatrix} \gamma_{11} & \gamma_{12} & \gamma_{13} \\ & \gamma_{22} & \gamma_{23} \\ & & \gamma_{33} \end{bmatrix} \omega_2 \tag{28}$$

In the present research, when the piezoelectric microplate is subjected to the impulsive loading, the Kachanvo damage evolution law [22] is adopted for an arbitrary point i in the piezoelectric plate with damage.

$$\frac{\partial \omega^i_2}{\partial t} = \begin{cases} B\left(\frac{|\sigma^i_{eq}|}{1-\omega^i_2} - \mu\sigma_f\right)^m & \left|\sigma^i_{eq}\right| \geq \mu(1-\omega^i_2)\sigma_f \\ 0 & \left|\sigma^i_{eq}\right| < \mu(1-\omega^i_2)\sigma_f \end{cases} \tag{29}$$

where B, m, and μ are the material constants, σ_{eq} is an equivalent stress which is based on certain failure criterion, σ_{f} is the stress of fatigue limit. From Equation (29), it can be

noticed that the damage will be triggered when the value of equivalent stress reaches the critical stress irrespective of tension or compression.

When the piezoelectric plate is subjected to n cyclic times of impulsive loading, the fatigue damage accumulation is employed by the Chaboche fatigue damage model [23].

$$\left(\frac{\delta D_i}{\delta N}\right)_n = \begin{cases} \oint_t \frac{\mathrm{d}\omega_2^i}{\mathrm{d}t}\mathrm{d}t & \left|\sigma_{eq}^i\right| \geq \mu(1-\omega_2^i)\sigma_f \\ 0 & \left|\sigma_{eq}^i\right| < \mu(1-\omega_2^i)\sigma_f \end{cases} \tag{30}$$

where D_i is the accumulative fatigue damage of an arbitrary point i under cyclic impulsive loads.

The relations between the electric fields E_x , E_y , E_z and the electric potential ϕ in the Cartesian coordinate system are defined by

$$E_x = -\phi_{,x}, \quad E_y = -\phi_{,y}, \quad E_z = -\phi_{,z} \tag{31}$$

For the piezoelectric plate in this paper, only electric field along the thickness direction E_z is considered. If the voltage is applied to the piezoelectric plate along the thickness direction only, then we have

$$E_z = V_e/h \tag{32}$$

where V_e is the applied voltage across the thickness of piezoelectric plates.

2.2. *Basic equations of piezoelectric microplates*

Now, consider a piezoelectric microplate with transverse cracks having thickness h, length a in the x-direction, width b in the y-direction subjected to a concentrated impulsive transverse load $q(t)$ shown in Figure 2. The reference surface defined by $z = 0$ is set on the middle surface of the undeformed plate. The principle directions of the material are assumed to coincide with the coordinated axis x, y, and z.

The concentrated impulsive transverse load $q(t)$ can be expressed as follows:

$$q(t) = \begin{cases} q_0 \sin(\frac{\pi t}{t_0}) & (k-1)T < t \leq t_0 + (k-1)T \\ 0 & kT - t_0 < t < kT \end{cases} (k = 1, 2, \ldots) \tag{33}$$

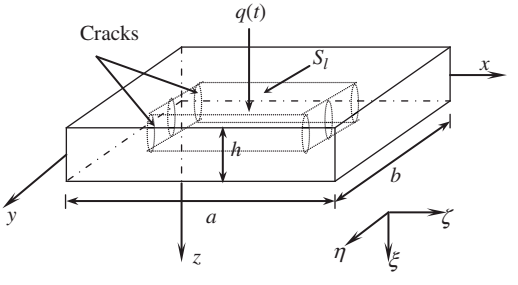

Figure 2. Geometric configuration of a piezoelectric microplate with transverse cracks under impulsive loading.

Assuming u , v, and w as the displacement components of an arbitrary point on the midsurface of the plate along the direction of x , y, and z, respectively. According to classical nonlinear theory, the strain components ε_x^0 , ε_y^0, and γ_{xy}^0 of the midsurface can be written as:

$$\varepsilon_x^0 = u_{,x} + \tfrac{1}{2}w_{,x}^2\, \varepsilon_y^0 = v_{,y} + \tfrac{1}{2}w_{,y}^2,\ \gamma_{xy}^0 = u_{,y} + v_{,x} + w_{,x}w_{,y} \tag{34}$$

and the curvatures κ_x, κ_y, and κ_{xy} of midsurface as:

$$\kappa_x = -w_{,xx}\ ,\quad \kappa_y = -w_{,yy}\ ,\quad \kappa_{xy} = -2w_{,xy} \tag{35}$$

Then the nonlinear strain–displacement relations are expressed as follows:

$$\varepsilon_x = \varepsilon_x^0 + z\kappa_x\ , \varepsilon_y = \varepsilon_y^0 + z\kappa_y\ , \gamma_{xy} = \gamma_{xy}^0 + z\kappa_{xy} \tag{36}$$

Suppose the damage variable remains constant through the thickness of plate. Denote $N_x, N_y,$ and N_{xy} as the membrane stress resultants and $M_x, M_y,$ and M_{xy} as the stress couples of the plate. According to the classical nonlinear plate theory, the nonlinear governing equations of motion for the piezoelectric plate can be written as:

$$\begin{aligned}
&N_{x,x} + N_{xy,y} = 0\\
&N_{xy,x} + N_{y,y} = 0\\
&M_{x,xx} + 2M_{xy,xy} + M_{y,yy} + N_x w_{,xx} + 2N_{xy}w_{,xy} + N_y w_{,yy}\\
&\qquad + q(t)\delta(x - a/2)\delta(y - b/2) = \rho h w_{,tt}
\end{aligned} \tag{37}$$

where ρ is the density of piezoelectric plate, $\delta(x)$ is the Dirac function and according to the classical plate theory and using Equations (22) and (36), the following constitutive equations can be obtained.

$$\begin{Bmatrix} N_x \\ N_y \\ N_{xy} \end{Bmatrix} = \int_{-h/2}^{h/2} \begin{Bmatrix} \sigma_x \\ \sigma_y \\ \sigma_{xy} \end{Bmatrix} dz = \begin{bmatrix} A_{11} & A_{12} & 0 \\ & A_{22} & 0 \\ & & A_{66} \end{bmatrix} \begin{Bmatrix} \varepsilon_x^0 \\ \varepsilon_y^0 \\ \gamma_{xy}^0 \end{Bmatrix} - \begin{Bmatrix} N_x^p \\ N_y^p \\ N_{xy}^p \end{Bmatrix} \tag{38}$$

$$\begin{Bmatrix} M_x \\ M_y \\ M_{xy} \end{Bmatrix} = \int_{-h/2}^{h/2} z \begin{Bmatrix} \sigma_x \\ \sigma_y \\ \sigma_{xy} \end{Bmatrix} dz = \begin{bmatrix} D_{11} & D_{12} & 0 \\ & D_{22} & 0 \\ & & D_{66} \end{bmatrix} \begin{Bmatrix} \kappa_x \\ \kappa_y \\ \kappa_{xy} \end{Bmatrix} - \begin{Bmatrix} M_x^p \\ M_y^p \\ M_{xy}^p \end{Bmatrix} \tag{39}$$

where N_x^p, N_x^p, N_{xy}^pandM_x^p, M_y^p, M_{xy}^p represent the component resultants and couples due to the piezoelectric effect, respectively. The stiffness coefficients A_{ij} and $D_{ij}(i,j = 1,2,6)$ of the piezoelectric plate are defined as follows:

$$A_{ij} = \int_{-h/2}^{h/2} C_{ij}\mathrm{d}z\ ,\quad D_{ij} = \int_{-h/2}^{h/2} z^2 C_{ij}\mathrm{d}z \quad (i,j = 1,2,6) \tag{40}$$

The resultants and couples due to the piezoelectric effect can be written as:

$$N_x^p = \int_{-h/2}^{h/2} e_{31}^1 \frac{V_e}{h} \mathrm{d}z, \quad N_y^p = \int_{-h/2}^{h/2} e_{32}^1 \frac{V_e}{h} \mathrm{d}z, \quad N_{xy}^p = 0$$
$$M_x^p = 0, \qquad M_y^p = 0, \qquad M_{xy}^p = 0 \tag{41}$$

Introduce the following dimensionless parameters:

$$\xi = \frac{x}{a}, \ \eta = \frac{y}{b}, \ U = \frac{u}{a}, \ V = \frac{v}{b}, \ W = \frac{w}{h}, \ \overline{A}_{11} = \frac{A_{11}}{C_{11}^* h}, \ \overline{A}_{12} = \frac{A_{12}}{C_{11}^* h}, \ \overline{A}_{22} = \frac{A_{22}}{C_{11}^* h},$$
$$\overline{A}_{66} = \frac{A_{66}}{C_{11}^* h}, \ \lambda_1 = \frac{h}{a}, \lambda_2 = \frac{h}{b}, \ \overline{D}_{11} = \frac{D_{11}}{C_{11}^* h^3} \ \overline{D}_{12} = \frac{D_{12}}{C_{11}^* h^3}, \ \overline{D}_{22} = \frac{D_{22}}{C_{11}^* h^3}, \ \overline{D}_{66} = \frac{D_{66}}{C_{11}^* h^3},$$
$$\overline{C}_{12} = \frac{C_{12}}{C_{11}^*}, \ \overline{C_{22}} = \frac{C_{22}}{C_{11}^*}, \ \overline{\sigma}_{eq} = \frac{\sigma_{eq}}{C_{11}^*}, \ \overline{\sigma}_f = \frac{\sigma_f}{C_{11}^*}, \ \overline{\alpha}_{11} = \frac{\alpha_{11}}{C_{11}^*}, \ \overline{\alpha}_{12} = \frac{\alpha_{12}}{C_{11}^*}, \ \overline{\alpha}_{22} = \frac{\alpha_{22}}{C_{11}^*},$$
$$\overline{\alpha}_{66} = \frac{\alpha_{66}}{C_{11}^*}, \ \overline{e_{31}^1} = \frac{e_{31}^1}{e_{31}^*}, \ \overline{e_{32}^1} = \frac{e_{32}^1}{e_{31}^*}, \ \overline{\beta}_{31} = \frac{\beta_{31}}{e_{31}^*}, \ \overline{\beta}_{32} = \frac{\beta_{32}}{e_{31}^*}, \ \bar{z} = \frac{z}{h},$$

$$\tau = \frac{t}{h}\sqrt{\frac{C_{11}^*}{\rho}}, \ \bar{t}_0 = \frac{t_0}{h}\sqrt{\frac{C_{11}^*}{\rho}}, \ \overline{q_0} = \frac{q_0}{C_{11}^*}, \ \overline{V_e} = \frac{e_{31}^* V_e}{C_{11}^* h} \tag{42}$$

By using Equations (22), (34)–(39), and (42), the dimensionless nonlinear governing equations of piezoelectric plate with initial damage are obtained and expressed in terms of U, V, and W as follows:

$$\overline{A}_{11,\xi}(U_{,\xi} + \tfrac{1}{2}\lambda_1^2 W_{,\xi}^2) + \overline{A}_{11}(U_{,\xi\xi} + \lambda_1^2 W_{,\xi} W_{,\xi\xi}) + \overline{A}_{12,\xi}(V_{,\eta} + \tfrac{1}{2}\lambda_2^2 W_{,\eta}^2)$$
$$+ \overline{A}_{12}(V_{,\xi\eta} + \lambda_2^2 W_{,\eta} W_{,\xi\eta}) + \tfrac{\lambda_2}{\lambda_1}\overline{A}_{66,\eta}(\tfrac{\lambda_2}{\lambda_1} U_{,\eta} + \tfrac{\lambda_1}{\lambda_2} V_{,\xi} + \lambda_1\lambda_2 W_{,\xi} W_{,\eta})$$
$$+ \overline{A}_{66}(\tfrac{\lambda_2^2}{\lambda_1^2} U_{,\eta\eta} + V_{,\xi\eta} + \lambda_2^2 W_{,\eta} W_{,\xi\eta} + \lambda_2^2 W_{,\xi} W_{,\eta\eta}) - \overline{e_{31,\xi}^1}\,\overline{V_e} = 0$$
$$\overline{A}_{12,\eta}(U_{,\xi} + \tfrac{1}{2}\lambda_1^2 W_{,\xi}^2) + \overline{A}_{12}(U_{,\xi\eta} + \lambda_1^2 W_{,\xi} W_{,\xi\eta}) + \overline{A}_{22,\eta}(V_{,\eta} + \tfrac{1}{2}\lambda_2^2 W_{,\eta}^2)$$
$$+ \overline{A}_{22}(V_{,\eta\eta} + \lambda_2^2 W_{,\eta} W_{,\eta\eta}) + \tfrac{\lambda_1}{\lambda_2}\overline{A}_{66,\xi}(\tfrac{\lambda_2}{\lambda_1} U_{,\eta} + \tfrac{\lambda_1}{\lambda_2} V_{,\xi} + \lambda_1\lambda_2 W_{,\xi} W_{,\eta})$$
$$+ \overline{A}_{66}(U_{,\xi\eta} + \tfrac{\lambda_1^2}{\lambda_2^2} V_{,\xi\xi} + \lambda_1^2 W_{,\eta} W_{\xi\xi} + \lambda_1^2 W_{,\xi} W_{,\xi\eta}) - \overline{e_{32,\xi}^1}\,\overline{V_e} = 0$$
$$- \lambda_1^4(\overline{D}_{11,\xi\xi} W_{,\xi\xi} + 2\overline{D}_{11,\xi} W_{,\xi\xi\xi} + \overline{D}_{11} W_{,\xi\xi\xi\xi}) - \lambda_1^2\lambda_2^2(\overline{D}_{12,\xi\xi} W_{\eta\eta} + 2\overline{D}_{12,\xi} W_{,\xi\eta\eta}$$
$$+ \overline{D}_{12} W_{,\xi\xi\eta\eta}) - 4\lambda_1^2\lambda_2^2(\overline{D}_{66,\xi\eta} W_{,\xi\eta} + \overline{D}_{66,\xi} W_{,\xi\eta\eta} + \overline{D}_{66,\eta} W_{,\xi\xi\eta} + \overline{D}_{66} W_{,\xi\xi\eta\eta})$$
$$- \lambda_1^2\lambda_2^2(\overline{D}_{12,\eta\eta} W_{,\xi\xi} + 2\overline{D}_{12,\eta} W_{\xi\xi\eta} + \overline{D}_{12} W_{,\xi\xi\eta\eta}) - \lambda_2^4(\overline{D}_{22,\eta\eta} W_{,\eta\eta} + 2\overline{D}_{22,\eta} W_{,\eta\eta\eta}$$

$$+\overline{D}_{22}W_{,\eta\eta\eta\eta}) + \lambda_1^2[\overline{A}_{11}(U_{,\xi} + \tfrac{1}{2}\lambda_1^2 W_{,\xi}^2) + \overline{A}_{12}(V_{,\eta} + \tfrac{1}{2}\lambda_2^2 W_{,\eta}^2) - \overline{e_{31}^1}\,\overline{V_e}]W_{,\xi\xi}$$

$$+ 2\lambda_1\lambda_2\overline{A}_{66}(\tfrac{\lambda_2}{\lambda_1}U_{,\eta} + \tfrac{\lambda_1}{\lambda_2}V_{,\xi} + \lambda_1\lambda_2 W_{,\xi}W_{,\eta})W_{,\xi\eta} + \lambda_2^2[\overline{A}_{12}(U_{,\xi} + \tfrac{1}{2}\lambda_1^2 W_{,\xi}^2)$$

$$+ \overline{A}_{22}(V_{,\eta} + \tfrac{1}{2}\lambda_2^2 W_{,\eta}^2) - \overline{e_{32}^1}\,\overline{V_e}]W_{,\eta\eta} + \overline{q}_0 \sin(\pi\tau/\bar{t}_0)\delta(\xi - 1/2)\delta(\eta - 1/2) = W_{,\tau\tau} \quad (43)$$

Suppose the boundary of the piezoelectric plate is simply immovably supported, the dimensionless boundary conditions can be expressed as:

$$\begin{aligned}
&\xi = 0,\ 1: \quad V = 0,\ \overline{A}_{11}(U_{,\xi} + \tfrac{1}{2}\lambda_1^2 W_{,\xi}^2) - \overline{e_{31}^1}\,\overline{V_e} = 0\\
&W = 0, \quad W_{,\xi\xi} = 0,\\
&\eta = 0,\ 1: \ U = 0,\ \overline{A}_{22}(V_{,\eta} + \tfrac{1}{2}\lambda_2^2 W_{,\eta}^2) - \overline{e_{32}^1}\,\overline{V_e} = 0\\
&W = 0, \quad W_{,\eta\eta} = 0
\end{aligned} \quad (44)$$

The dimensionless damage evolution equation under one cyclic impulsive loading and fatigue damage accumulation equation under $n$cyclic impulsive loading can be written respectively as follows:

$$\frac{\partial\omega_2^i}{\partial\tau} = \begin{cases} \bar{B}\left(\frac{|\bar{\sigma}_{\text{eq}}^i|}{1-\omega_2^i} - \mu\overline{\sigma}_f\right)^m & |\bar{\sigma}_{\text{eq}}^i| \geq \mu(1-\omega_2^i)\bar{\sigma}_f \\ 0 & |\bar{\sigma}_{\text{eq}}^i| < \mu(1-\omega_2^i)\bar{\sigma}_f \end{cases} \quad (45)$$

$$\left(\frac{\delta D_i}{\delta N}\right)_n = \begin{cases} \oint_\tau \frac{\mathrm{d}\omega_2^i}{\mathrm{d}\tau} d\tau & |\bar{\sigma}_{\text{eq}}^i| \geq \mu(1-\omega_2^i)\overline{\sigma}_f \\ 0 & |\bar{\sigma}_{\text{eq}}^i| < \mu(1-\omega_2^i)\overline{\sigma}_f \end{cases} \quad (46)$$

Taking the midsurface normal stress of the piezoelectric plate as the equivalent stress $\overline{\sigma}_{\text{eq}}$ that is vertical to the axis z direction, it can be presented as

$$\bar{\sigma}_{\text{eq}} = \overline{C}_{12}(U_{,\xi} + \tfrac{1}{2}\lambda_1^2 W_{,\xi}^2 - \lambda_1^2\bar{z}W_{,\xi\xi}) + \overline{C}_{22}(V_{,\eta} + \tfrac{1}{2}\lambda_2^2 W_{,\eta}^2 - \lambda_2^2\bar{z}W_{,\eta\eta}) - \overline{e_{32}^1}\,\overline{V_e} \quad (47)$$

3. Solution methodology

To seek the approximate solutions of governing Equation (43), which satisfies the boundary conditions in Equation (44), the unknown functions U, V, and W are separated both for space and time. The finite difference method is used for space, and the partial derivatives with respect to the space coordinate variables are replaced by difference form. The time τ is equally divided into small time segments $\Delta\tau$, and the whole equations are iterated to seek solutions. At each step of the iteration, the nonlinear items in the equations and the boundary conditions are linearized. For example, at the step J, the nonlinear items may be transformed to

$$(x \cdot y)_J = (x)_J \cdot (y)_{J_p} \quad (48)$$

where $(y)_{J_p}$ is the average value of those obtained in the preceding two iterations. For the initial step of the iteration, it can be determined by using the quadratic extrapolation, i.e.,

$$(y)_{J_p} = A(y)_{J-1} + B(y)_{J-2} + C(y)_{J-3} \tag{49}$$

and for the different step of the iteration, the coefficients A, B, and C can be expressed as follows:

$$\begin{aligned} J = 1: \ & A = 1, B = 0, C = 0 \\ J = 2: \ & A = 2, B = -1, C = 0 \\ J \geq 3: \ & A = 3, B = -3, C = 1 \end{aligned} \tag{50}$$

Moreover, using the Newmark scheme, the inertia in Equation (43) can be expressed as follow:

$$\begin{aligned} (W_{,\tau\tau})_J &= \frac{4(W_J - W_{J-1})}{(\Delta\tau)^2} - \frac{4(W_{,\tau})_{J-1}}{\Delta\tau} - (W_{,\tau\tau})_{J-1} \\ (W_{,\tau})_J &= (W_{,\tau})_{J-1} + \tfrac{1}{2}[(W_{,\tau\tau})_{J-1} + (W_{,\tau\tau})_J]\Delta\tau \\ W_J &= W_{J-1} + (W_{,\tau})_{J-1}\Delta\tau + \tfrac{1}{4}[(W_{,\tau\tau})_{J-1} + (W_{,\tau\tau})_J](\Delta\tau)^2 \end{aligned} \tag{51}$$

For every time step, if the iteration lasts until the difference of the present value and the former is smaller than 0.1%, then continue the calculation of the next step.

With respect to fatigue damage accumulation variables D_i, it is impossible to analyze the micro-damage accumulation under multimillions cyclic impulsive loads. In order to save the time, the cyclic skip method is employed [24]; that is, the cyclic strain–stress analysis is not applied in the quasi-stable state. Under a certain segmentation of cyclic loads (the corresponding cyclic number ΔN_k), the micro-damage accumulation $\left(\delta D_i / \delta N\right)_k$ is considered to be constant. Usually, ΔN_k is taken as follows:

$$\Delta N_k = \frac{\overline{\Delta D}}{\left(\delta D_i / \delta N\right)_{k(M^*)}} \tag{52}$$

where $\overline{\Delta D}$ is the average fatigue damage accumulation at the point M^* of maximum damage in the plate.

As to the next stage cyclic N_{k+1}, the fatigue damage of an arbitrary point i is given as follows:

$$\begin{aligned} N_{k+1} &= N_k + \Delta N_k \\ (D_{k+1})_i &= (D_k)_i + \left(\frac{\delta D_i}{\delta N}\right)_k \Delta N_k \end{aligned} \tag{53}$$

4. Numerical results

4.1. Comparison study

To ensure the accuracy and effectiveness of the present method, two test examples were performed for free vibrations of the piezoelectric microplate without considering damage

effect and nonlinear dynamic response of isotropic plates without considering piezo-effect and damage effect.

Example 1. The effect of thickness-span ratio (h/a) on the fundamental frequencies of piezoelectric plate without damage is investigated. Consider a piezoelectric plate consisting of PZT-4A layers under the short-circuited electrical condition. The material properties [25] for PZT-4A are given as follows:

$$\begin{aligned}
&c_{11} = 13.2 \times 10^{10}(\mathrm{N/m^2}),\ \ c_{12} = 7.1 \times 10^{10}(\mathrm{N/m^2}),\ \ c_{13} = 7.3 \times 10^{10}(\mathrm{N/m^2}),\\
&c_{33} = 11.5 \times 10^{10}(\mathrm{N/m^2}),\ \ c_{44} = 2.6 \times 10^{10}(\mathrm{N/m^2}),\ \ c_{66} = 3.0 \times 10^{10}(\mathrm{N/m^2}),\\
&e_{15} = 10.5(\mathrm{C/m^2}),\ \ e_{31} = -4.1(\mathrm{C/m^2}),\ \ e_{33} = 14.1(\mathrm{C/m^2}),\ \ \rho = 7.5 \times 10^{3}(\mathrm{kg/m^3})\\
&\kappa_{11} = 7.124 \times 10^{-9}(\mathrm{F/m}),\ \ \kappa_{33} = 5.841 \times 10^{-9}(\mathrm{F/m}) \qquad (54)
\end{aligned}$$

The non-dimensional fundamental frequencies $\overline{\Omega}$ ($\overline{\Omega} = \Omega a\sqrt{\rho/C_{11}^*}$) are calculated and compared in Table 1 with three-dimensional (3-D) solutions. Ω is the fundamental frequency of the piezoelectric plate. Table 1 shows that the results are satisfactory up to 3-D solutions validity limit, but larger than it because the nonlinear items in nonlinear dynamic equations are linearized in the solution methodology.

Example 2. The present problem is simplified and is suitable for nonlinear dynamic response analysis for isotropic rectangular microplate without considering piezo-effect and damage effect. A simply supported movable microplate having the same thickness and material constants is considered. The material parameters and geometric parameters are given as

$$C_{66}/C_{22} = 1, C_{11}/C_{22} = 10,\ C_{12}/C_{22} = 0.3, \lambda_1 = 0.1,\ \lambda_2 = 0.1$$

And the transverse load is taken as $\overline{q} = f_0 \sin\theta\tau \sin\pi\xi \sin\pi\eta$ ($f_0 = 0.004$, $\theta = 0.01$). The response curve of the center deflection W_0 versus time for isotropic plate is presented in Figure 3, and compared with the results from FEM. The close agreements between the present results and those of the FEM solution demonstrate that the present method is accurate and effective.

Table 1. Comparison of non-dimensional fundamental frequencies of piezoelectric plate under different thickness-span ratios.

	$h/a = 0.01$		$h/a = 0.1$	
a/b	3-D (Ref. [22])	Present	3-D (Ref. [22])	Present
1	0.0514	0.0526	0.4969	0.5123
2	0.1287	0.1308	1.1863	1.2256

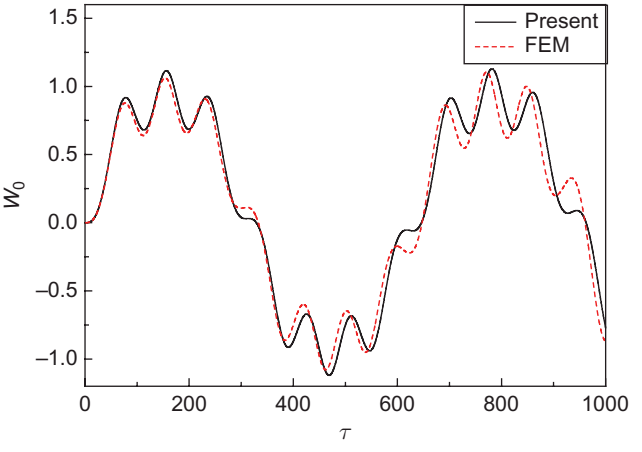

Figure 3. Non-linear dynamic response of center deflection versus time for isotropic plate.

4.2. *Parametric study*

A piezoelectric plate consisting of the PZT-4A, including initial damage, is considered in this section. In all examples, the geometric parameters are given as $\lambda_1 = 0.1$ and $\lambda_2 = 0.1$. When the damage effect is in consideration, the material parameters related to damage in all examples are taken as:

$$\overline{B} = 0.5,\ n = 1.1,\ \overline{\sigma}_f = 1.8 \times 10^{-3}, \overline{\alpha_{11}} = -0.05, \overline{\alpha_{12}} = -0.05, \overline{\alpha_{22}} = -0.05,$$

$$\overline{\alpha_{66}} = -0.05, \overline{\beta_{31}} = -0.05, \overline{\beta_{32}} = -0.05, \mu = 0.6.$$

Figure 4 shows the fatigue damage life curve *D*–*N* of piezoelectric plate with initial damage under different cyclic impulsive loads. *D* is taken as the value of the maximum damage point in the piezoelectric plate and *N* is the total cyclic number of impulsive loads. The electrical load is given as $\overline{V_e} = 0$. It can be seen that when the amplitude of impulsive loads increases, the fatigue damage life decreases and that the fatigue damage variable *D* increases with the increment of the total cyclic number *N*. As indicated in Figure 4, the increase of the amplitude of impulsive loads leads to the increment of the stress level of any point in the piezoelectric plate, which can correspondingly result in the higher rate of fatigue damage accumulation.

The diagrams of fatigue damage life related to the total cyclic number of impulsive loads for different electrical loads are shown in Figure 5. The amplitude of the impulsive load is taken as $\overline{q}_0 = 0.3$. According to the results, fatigue damage life as a function of electrical loads can be estimated. It can be seen that the positive voltage results in the longer fatigue life, while the negative voltage leads to the faster degradation of fatigue damage life. It can be concluded from the results that the positive voltage acting upon the piezoelectric plate with damage is equivalent to a compression piezoelectric force acting in the out-of-plane direction of the plate to a certain extent, which leads to the slower degradation rate of fatigue life.

Figure 6 shows the relations of fatigue damage variables *D*, the cyclic number *N*, and the distance of the center to any point of the plate ζ. The amplitude of the impulsive load and the electrical load are taken as $\overline{q}_0 = 0.3$ and $\overline{V_e} = 0$, respectively. It can be illustrated

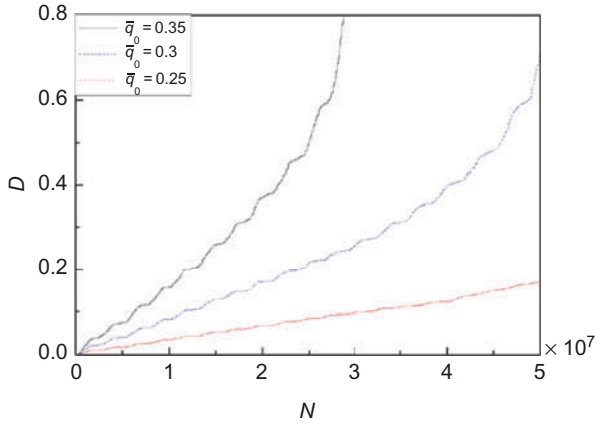

Figure 4. Effect of cyclic impulsive loads on the fatigue damage life curve $D - N$.

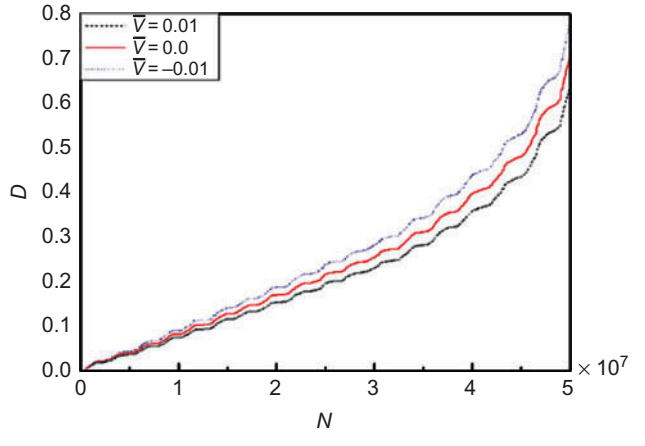

Figure 5. Effect of electrical loads on the fatigue damage life curve $D - N$.

that the fatigue damage variable increases gently when the number of the repeated times is below the value of 10^7, and that the fatigue damage variable decreases with the increase of the distance of the center to any point in the plate. Due to the unsteady vibration under cyclic impulsive loads, the fatigue damage evolution and fatigue damage accumulation become different.

Figure 7 shows the degradation of elastic constants with respect to the cyclic number N. In Figure 7, the amplitude of the impulsive load and the electrical load are taken as $\overline{q}_0 = 0.3$ and $\overline{V_e} = 0$, respectively. It can be seen that the variation of elastic constant C_{66} with respect to the cyclic number is linear, whereas all other elastic constants vary non-linearly, as the number of cyclic loads increases. Elastic constant C_{11} is the most sensitive to damage, which affects the response of the piezoelectric materials in the plane of the piezoelectric, and therefore is important when piezoelectric ceramic wafers are used as actuators in the smart structures.

Figure 8 shows the effect of the amplitude of the impulsive loads on the elastic constant under the different cyclic number of impulsive loads. The electrical load is given as $\overline{V_e} = 0$. It can be seen from Figure 8 that the increment of the amplitude of impulsive loads

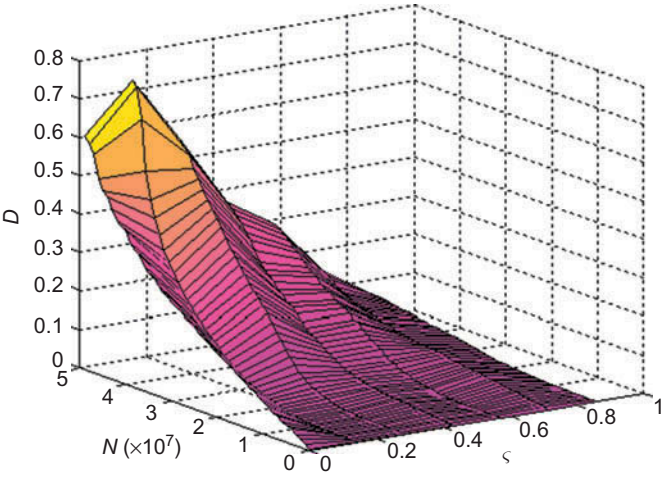

Figure 6. Relations of fatigue damage variables, cyclic number, and distance of the center to any point of the plate.

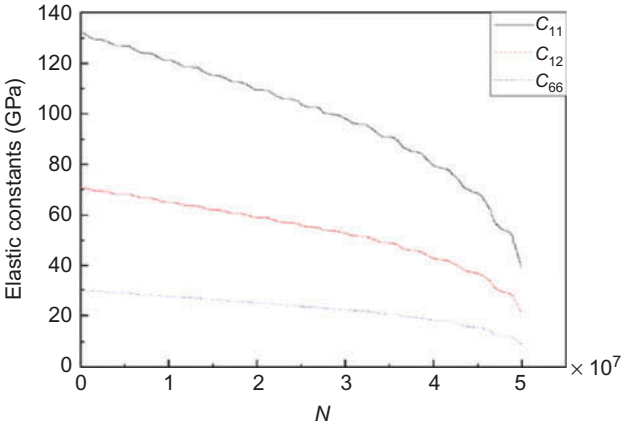

Figure 7. Effective elastic constants versus cyclic number of impulsive loadings.

results in a higher degradation rate of elastic constants. It can be concluded that the larger amplitude of the impulsive loads leads to the larger stress level in the in-plane direction of the piezoelectric plate, thereby resulting in the higher degradation rate of elastic constants.

Figure 9 shows the effect of the electric loads on the elastic constant under different number of cyclic impulsive loads. The amplitude of the impulsive load is taken as $\overline{q}_0 = 0.3$. It can be illustrated that the positive voltage can slow down the degradation of elastic constants, whereas the negative voltage can accelerate the degradation rate of elastic constants. When the applied voltage is positive, a tensile piezoelectric force will be emerged in the in-plane direction of the plate, which will decrease the vibrating amplitude, the stress level of the plate, and the degradation rate of the fatigue damage variables.

Figures 10 and 11 show the degradation of piezoelectric constants and the degradation of permittivity of the piezoelectric plate with respect to the cyclic number of impulsive

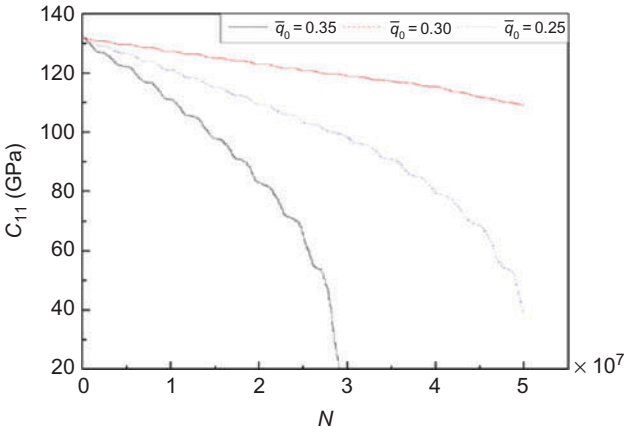

Figure 8. Effects of cyclic loadings on effective elastic constants under different cyclic number.

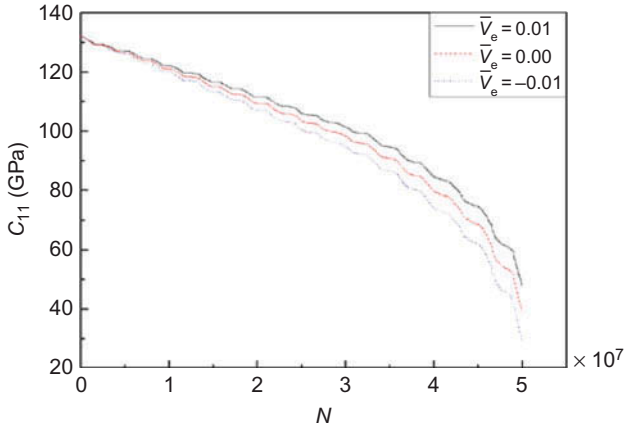

Figure 9. Effects of electrical loadings on effective elastic constants under different cyclic number.

loads, respectively. In these two figures, the amplitude of the impulsive load and the electrical load are taken as $\overline{q}_0 = 0.3$ and $\overline{V_e} = 0$, respectively. It can be seen from Figure 10 that the piezoelectric constants vary non-linearly, as the number of cyclic loads grows, and that the value of e_{13} increases with the cyclic number of impulsive loads. From Figure 11, it can be concluded that the permittivity of piezoelectric plate decreases and vary non-linearly with the repeated times of cyclic loads and that the values of $\kappa_{11}$and κ_{33} tend to be the same.

5. Conclusions

This article presents an approach to predict the fatigue damage life of piezoelectric microplate under cyclic impulsive loading using the Talreja's tensor-valued internal state damage variables and the Chaboche fatigue damage development equations. The effects of the transverse impulsive cyclic loads and the electrical loads on the fatigue life and the effective properties of piezoelectric plates have been investigated. Numerical results show that the amplitude of the impulsive loads has significant impact on the fatigue life

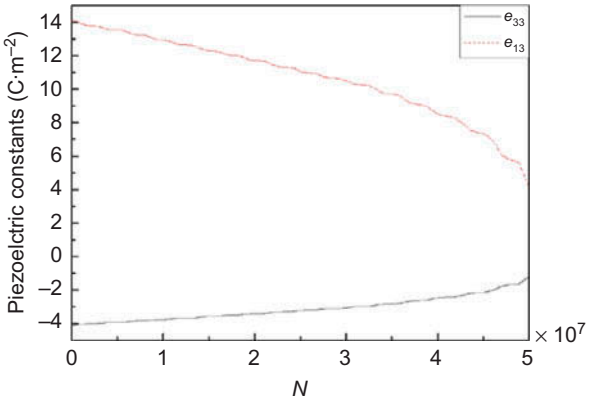

Figure 10. Effective piezoelectric constants versus cyclic number of impulsive loadings.

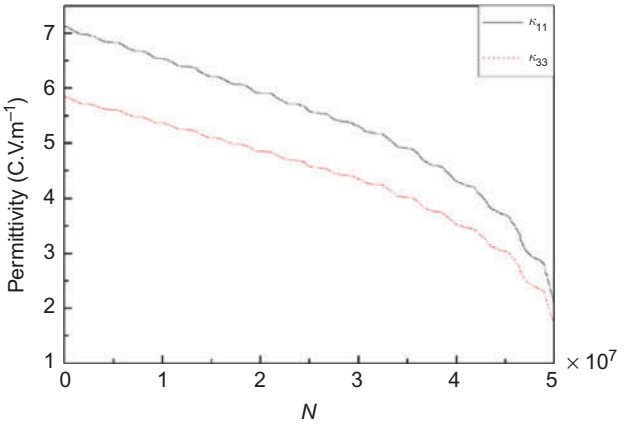

Figure 11. Effective permittivity versus cyclic number of impulsive loadings.

curve of the microstructure. When the amplitude of the cyclic loads increases, the vibrating amplitude of plate and the stress level in the in-plane direction of the plate increase correspondingly, thereby resulting in the higher degradation rate of fatigue life. It can be also concluded that when the applied voltage is positive, a tensile piezoelectric force is emerged in the in-plane direction of the plate, which decreases the amplitude of the structure and slows down the degradation rates of the fatigue life and material constants of piezoelectric structure. All these findings offer great insights to fabricate the piezoelectric-based microdevices suitable for harsh conditions and also enhance the service life of these devices.

No research, however, provides a perfect answer, with this work being no exception to the rule. Based on current assumptions employed in implementing fatigue damage analysis, more work remains to be done. Specifically, we only consider one damage mode in the specimen and the negligible sliding between crack faces, which means that there is no coupling effect between crack faces and damage modes. Thus, more theoretical work should be devoted to explore and complement the full spectrum of the multiple damage mode effects. The authors hope that this study can catalyze further work in the fatigue analysis of electronic microdevices.

References

[1] K.P. Chong and X.Q. Wang, *Research and challenges in converging technologies and multi-scale mechanics*. IMECE 2012–85553, ASME Congress, Houston, TX, 2012.

[2] J.T. Oden, *Simulation-based engineering science: Revolutionizing engineering science through simulation*, Report of the National Science Foundation Blue Ribbon Panel on Simulation-Based Engineering Science, K.P. Chong, cognizant program director, 2006.

[3] M. Buggy and G. Dillon, *Flexural fatigue of carbon fibre-reinforced PEEK laminates*, Composites 22 (1991), pp. 191–198.

[4] H. El Kadi and F. Ellyin, *Effect of stress ratio on the fatigue of unidirectional glass fibre/epoxy composite laminae*, Composites 25 (1994), pp. 917–924.

[5] B. Harris, H. Reiter, T. Adam, R.F. Dickson, and G. Fernando, *Fatigue behaviour of carbon fibre-reinforced plastics*, Composites 21 (1990), pp. 232–242.

[6] T. Nyman, *Composite fatigue design methodology: A simplified approach*, Compos. Struct. 35 (1996), pp. 183–194.

[7] C. Dahlen and G.S. Springer, *Delamination growth in composites under cyclic loads*, J. Compos. Mater. 28 (1994), pp. 732–781.

[8] G.M. Feng, A.J. Kinloch, and F.L. Mattews. *Development of a method for predicting the fatigue life of CFRP components*. International Conference on Fatigue of Composites: Pro, 3–5, Paris, France, 1997, pp. 407–414.

[9] R.D. Mindlin, *Forced thickness-shear and flexural vibrations of piezoelectric crystal plates*, J. Appl. Phys. 23 (1952), pp. 83–88.

[10] H.F. Tiersten, *Linear piezoelectric plate vibrations: Elements of the linear theory of piezoelectricity and the vibrations of piezoelectric plates*, Plenum Press, New York, 1969.

[11] K. Chandrashekhara and R. Tenneti, *Thermally induced vibration suppression of laminated plates with piezoelectric sensors and actuators*, Smart Mater. Struct. 4 (1995), p. 281.

[12] X. Zhou, A. Chattopadhyay, and H. Gu, *Dynamic responses of smart composites using a coupled thermo-piezoelectric-mechanical model*, AIAA J. 38 (2000), pp. 1939–1948.

[13] B.-T. Wang and C.A. Rogers, *Laminate plate theory for spatially distributed induced strain actuators*, J. Compos. Mater. 25 (1991), pp. 433–452.

[14] H.S. Tzou and M. Gadre, *Theoretical analysis of a multi-layered thin shell coupled with piezoelectric shell actuators for distributed vibration controls*, J. Sound Vib. 132 (1989), pp. 433–450.

[15] K. Xu, A.K. Noor, and Y.Y. Tang, *Three-dimensional solutions for free vibrations of initially-stressed thermoelectroelastic multilayered plates*, Comput. Methods Appl. Mech. Eng. 141 (1997), pp. 125–139.

[16] J.A. Mitchell and J.N. Reddy, *A refined hybrid plate theory for composite laminates with piezoelectric laminae*, Int. J. Solids Struct. 32 (1995), pp. 2345–2367.

[17] S.S. Rao and M. Sunar, *Piezoelectricity and its use in disturbance sensing and control of flexible structures: A survey*, Appl. Mech. Rev. 47 (1994), pp. 113–123.

[18] T.R. Tauchert, *Piezothermoplastic behavior of a laminated plate*, J. Therm. Stresses 15 (1992), pp. 25–37.

[19] R. Talreja, *Damage development in composites – Mechanisms and modeling*, J. Strain Anal. Eng. Des. 24 (1989), pp. 215–222.

[20] C.-c Wang and C. Truesdell, *Introduction to rational elasticity*, in *Mechanics of Continua*, H.G. Schöpf, ed., Noordhoff International Pub. Co., Leyden, 1973, xii, p. 556.

[21] A.C. Eringen, *Mechanics of Continua*, 2d ed., R. E. Krieger Pub. Co., Huntington, NY, 1980, xv, p. 592.

[22] L.M. Kachanov, *Introduction to continuum damage mechanics*, Martinus Nijhoff Publishers, Netherlands, 1986.

[23] J.L. Chaboche, *Continuum damage mechanics: Part I – General concepts, part II-damage growth, crack initiation, and crack growth*, J. Appl. Mech. 55 (1988), pp. 59–64.

[24] W. Van Paepegem, J. Degrieck, and P. De Baets, *Finite element approach for modelling fatigue damage in fibre-reinforced composite materials*, Compos. Part B Eng. 32 (2001), pp. 575–588.

[25] P. Cupiał, *Three-dimensional natural vibration analysis and energy considerations for a piezoelectric rectangular plate*, J. Sound Vib. 283 (2005), pp. 1093–1113.